

# Crystal Plasticity Analysis of Work Hardening Behavior at Large Strains in Ferritic Single Crystal

Akihiro UENISHI\*  
Natsuko SUGIURA  
Masaaki SUGIYAMA

Eiji ISOGAI  
Yoichi IKEMATSU  
Shunji HIWATASHI

## Abstract

*The material behavior at large strains is one of the most important properties in sheet steel, for it undergoes severe plastic deformation in its use. We focus on the relationship between the work hardening behavior at large strains and the evolution of microstructure during deformation by experimental and numerical methods, with attention to the crystal orientation. The work hardening behavior of ferritic single crystal with different orientations has been characterized by simple shear experiments. At the same time, TEM observations have been performed to study microstructures after shear deformation. The work hardening behavior depends largely on the crystal orientation. The observed microstructures may be classified into three types. The work hardening behavior could be correlated to the type of microstructure via the activity of slip systems. Crystal plasticity analysis revealed that the behavior in macroscopic and microscopic scales could be attributed to the activity of slip systems and their interaction.*

## 1. Introduction

The application of numerical analysis based on continuum mechanics has been rapidly expanding at actual development sites as an indispensable tool to predict product performance and formability. This movement is called digital development, and is largely contributing to the shortening of development periods and the optimization of materials/structures, etc. Steel sheet is one of the materials that are most commonly used in the fields in which new development techniques, like numerical analysis, are applied. The important characteristic of sheet steel is that it is subject to large deformation during the stamping process. Various types of high-strength steels have been developed and put to practical use. However, the actual perfor-

mance of those steels depends largely on their work hardening behavior at large strains.

The work hardening behavior of metallic materials has been studied extensively as a major theme of materials science. Concerning the work hardening behavior at large strains, there are interesting reports that relate characteristic work hardening behaviors to types of dislocation structure formed in the material.<sup>1-6)</sup> In addition, the recent numerical analysis technology that takes into account more microscopic deformation processes has reached such a level as to allow for correlating the structural change inside the material to an external response of the material such as work hardening behavior. Therefore, in the present study, we investigated the work hardening behavior of ferritic single crystals at large strains and carried out

---

\* Senior Researcher, Dr., Forming Technologies R&D Center, Steel Research Laboratories 20-1, Shintomi, Futttsu, Chiba 293-8511

numerical analysis using crystal plasticity models that take into account the interaction between slip systems.

## 2. Work Hardening Behavior of Ferritic Single Crystal at Large Strains

The material used in this study was a ferritic Fe-Cr alloy (mass%: 0.0017C, 16.45Cr, 0.10Ni). In order to grow grains, the material was annealed at 1,350°C for 72 h in Ar atmosphere. The work hardening behavior of the material was measured using a simple shear test.<sup>7,8)</sup> When evaluating the mechanical properties of materials, tensile tests are usually used. However, in tensile tests, necking or fracture of specimens tend to occur at lower strains. Therefore, it can hardly be employed to measure the work hardening behavior at large strains. On the other hand, simple shear tests, whereby a flat specimen is sheared in-plane, permit measuring the work hardening behavior at large strains without being affected by the necking of specimens.

After using the X-ray Laue method to identify the crystal orientation of each grain, we cut out single crystal planar specimens (thickness: 1 mm) with plane normal of {111}, {100}, and {110} and subjected those specimens to a simple shear test. In the test, for each of specimens, the representative shear direction was selected. Here, the test conditions are shown by a combination of plane normal { } and shear direction < >. **Table 1** shows the orientations of the single crystal specimens under the present test conditions. (In a simple shear test, the maximum shear stress plane is always perpendicular to both the sheet plane normal and shear direction.)

**Fig. 1** shows the shear stress-shear strain curves of single crystal specimens with different normal and shear directions by simple shear tests. The work hardening behavior has shown a large variety depending on the test conditions, even though the specimens were cut out from the identical material. Similar results were reported for single crystal experiments of uniaxial tensile tests. Namely, the critical resolved shear stress evaluated from the uniaxial tensile tests showed considerable dependence on the crystal orientations.<sup>9)</sup> However, in the case of simple shear tests, as long as the crystal orientation is properly selected, it is possible to measure the work hardening behavior without being influenced by crystal rotations even when the number of active slip systems is relatively small.

Looking at the behaviors of the individual specimens in detail, the specimen with the {111} plane normal and <112> shear direction (hereafter described as {111} <112>) shows work hardening even at large strains, although the work hardening rate is initially low. In contrast, the {100} <001> specimen shows an initial high work hardening rate but it saturates very quickly. The {100} <011> and {110} <001> specimens exhibit intermediate behavior between the two specimens. With the {100} <001> specimen whose work

hardening quickly saturated, even in simple shear deformation, making it impossible to accurately measure its work hardening behavior beyond 15%.

The {110} <112> and {110} <557> specimens show a two-stage hardening behavior in which the slope of the stress-strain curve changes halfway. **Fig. 2** shows the relationship between the slope of the stress-strain curve and the shear stress. It was found that while the slope for the {111} <112> specimen decreases with increased stress, the {110} <112> and {110} <557> specimens, which show a slope nearly the same as that of the {111} <112> specimen in the small-stress region during initial deformation, began increasing in slope halfway and became similar in behavior to the {100} <011> specimen. It was also found that with the {100} <001>, {100} <011> and {110} <001> specimens, the slope of the stress-strain curve is larger than that under any other test conditions.

As observed so far, the work hardening behavior of single crystal specimens varies markedly according to the plane normal orientation and shear direction of the crystals. This is considered due to the activities of different slip systems under various deformation conditions and the interaction of those slip systems. Therefore, we carried out deformation analysis using crystal plasticity models that permits taking into consideration the influence of slip systems.

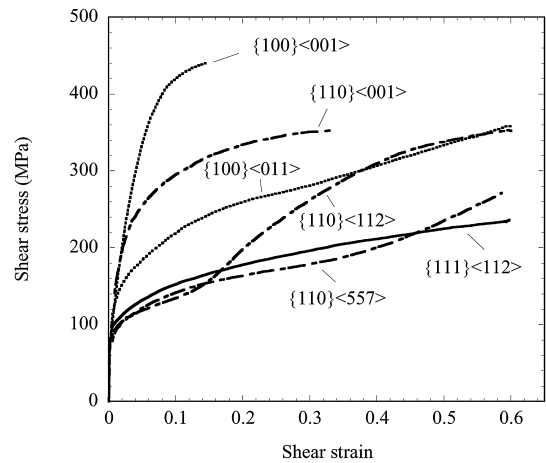


**Fig. 1** Shear stress vs. shear strain curves of ferritic single crystals

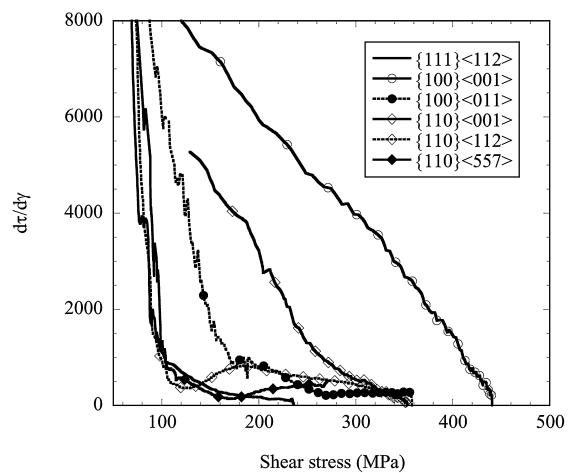


**Fig. 2** Slope of stress-strain curves vs. shear stress curves

**Table 1** Crystal orientation in single crystal specimens used for simple shear tests

Test conditions	Normal direction	Shear direction	Maximum shear stress plane
{111}<112>	(111)	$[\bar{1}\bar{1}2]$	( $\bar{1}\bar{1}0$ )
{100}<001>	(001)	$[0\bar{1}0]$	(100)
{100}<011>	(001)	$[1\bar{1}0]$	(110)
{110}<001>	(110)	$[001]$	( $\bar{1}\bar{1}0$ )
{110}<112>	( $\bar{1}\bar{1}0$ )	$[11\bar{2}]$	(111)
{110}<557>	( $\bar{1}\bar{1}0$ )	$[55\bar{7}]$	(7710)

### 3. Crystal Plasticity Analysis of Work Hardening Behavior at Large Strains

#### 3.1 Outline of crystal plasticity analysis

In macroscopic analysis of deformation behavior, the phenomenological (macroscopic) theory of plasticity using a yield function is normally applied. The crystal plasticity analysis assumes that the plastic deformation is a combination of shear (slip) deformations that occur only in the direction along the slip planes, as shown in Fig. 3.<sup>10)</sup> The characteristics of crystal plasticity analysis are: (1) the way the finite deformation correlates to the deformation of each slip system, (2) the way the activity/inactivity of each slip system is judged, and (3) the way the deformation produced in each slip system correlates to the total stress.

Concerning (1), the total deformation is expressed as the combination of shear deformations caused by the individual slip systems as described above. By resolving the velocity gradient tensor formed by that combination into the symmetric part and the asymmetric part, it is possible to obtain the plastic strain velocity and plastic spin in a natural way. This is one of the advantageous characteristics of the crystal plasticity analysis.<sup>10)</sup> For fcc metals, 12 slip systems of the {111} <110> type are used. For bcc metals, 24 slip systems of the {110} <111> and {112} <111> types or 48 slip systems (the prior 24 systems plus 24 systems of the {123} <111> type) are used.

With respect to (2), it is common practice to introduce the strain rate sensitivity of flow stress and give the activity, which is expressed as strain rate of each slip system, as a function of the flow stress, although there are various other approaches. It is well known that, a slip occurs when the shear stress acting upon a slip system exceeds a certain stress (critical shear stress). Of the various obstacles shown in Fig. 4, short range obstacles can be overcome by thermal activation process. Thus, the activity of each slip system can be defined as a frequency to overcome such obstacles. Therefore, all slip systems

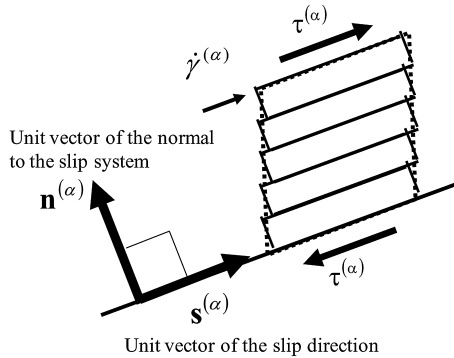


Fig. 3 Shear deformation and slip system

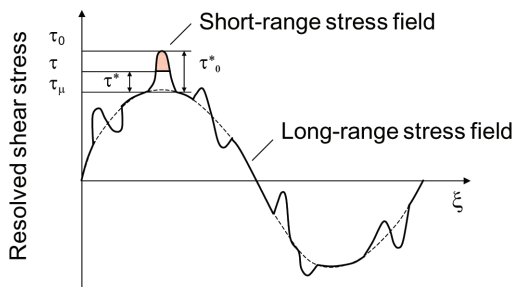


Fig. 4 Resolved shear stresses acting on a gliding dislocation

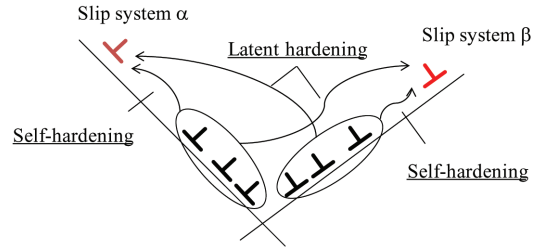


Fig. 5 Hardening due to interaction between slip systems

can be thought as potentially active systems, the overcome frequency, or the strain rate of each system, can be decided from the given flow stress. In this manner, it becomes possible to obtain the activity of each slip system without explicitly distinguishing between active slip systems and inactive ones. In the present study, we used the following equation.<sup>11)</sup>

$$\dot{\gamma}^{(\alpha)} = \dot{\gamma}_0 \operatorname{sgn}(\tau^{(\alpha)}) \left| \frac{\tau^{(\alpha)}}{g^{(\alpha)}} \right|^{1/m} \quad (1)$$

Where  $\dot{\gamma}^{(\alpha)}$  denotes the strain rate of slip system  $\alpha$ ;  $\tau^{(\alpha)}$ , the flow stress acting on slip system  $\alpha$ ;  $m$ , the strain rate sensitivity index; and  $\dot{\gamma}_0$ , the reference strain rate.  $g^{(\alpha)}$  prescribes the relationship between flow stress and strain rate for each slip system. As can be seen from the fact that the strain rate becomes small when  $g^{(\alpha)}$  becomes large,  $g^{(\alpha)}$  is related to the work hardening of the material.

With respect to (3), by considering the equation for the evolution of  $g^{(\alpha)}$ , it is possible to correlate it with the total work hardening. The general equation is given as follows.

$$\dot{g}^{(\alpha)} = \sum_{\beta} h_{\alpha\beta} |\dot{\gamma}^{(\beta)}| \quad (2)$$

Fig. 5 shows the interaction between slip systems. The flow stress in a given material is the sum of the flow stresses acting on mobile dislocations in each slip system. It can be divided into self-hardening from dislocations, which belong to the same slip system and latent hardening from dislocations, which in turn belong to other slip systems. In the above equation,  $h_{\alpha\beta}$  is the hardening matrix that indicates the interaction between slip systems. Specifically, the matrix indicates the contribution of slip  $\dot{\gamma}^{(\beta)}$  of system  $\beta$  in the hardening of system  $\alpha$ . The diagonal components of the matrix represent self-hardening and the nondiagonal components represent latent-hardening. For  $h_{\alpha\beta}$ , many different models have been proposed. In the present study, we used the following equation.

$$h_{\alpha\beta} = qh(\gamma_i) + (1 - q)h(\gamma_j)\delta_{\alpha\beta} \quad (3)$$

Where  $\delta_{\alpha\beta}$  is Kronecker delta;  $q$ , a constant indicating the level of latent-hardening; and  $h(\gamma_i)$ , the reference work hardening rate.

By using the above framework, it is possible to make a calculator, which gives the macroscopic stress/strain as the combination of shear deformations of the slip systems.

#### 3.2 Results of crystal plasticity analysis of single crystal deformed by simple shear

In order to make numerical analysis based on the simple shear tests of single crystal specimens shown in Fig. 1, we used one-element model assuming plane strain condition with reduced integration element. The work hardening rate,  $h(\gamma_i)$ , in Equation (3) was determined using experimental data obtained with the {110} <001> specimen. Considering that the work hardening rate represents the pure contribution of accumulated dislocations without interaction between slip systems, we selected {110} <001> specimens since they

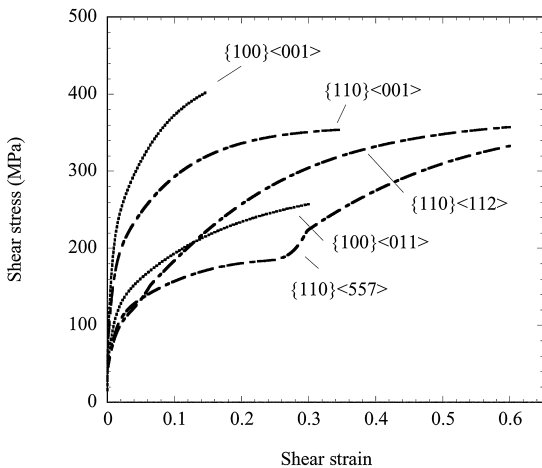


Fig. 6 Shear stress vs. shear strain curves of ferritic single crystals obtained by crystal plasticity analysis

are free from crystal rotations due to deformation during the shear test and their slip planes are in parallel with the shear direction. In addition, to express sharp changes in the work hardening rate, we used the following extended version of the equation of Voce et al.<sup>12)</sup>

$$h(\gamma_i) = C_1 g_1 e^{-C_1 \gamma_i} + C_2 g_2 e^{-C_2 \gamma_i} \quad (4)$$

( $g_1 = 108\text{MPa}$ ,  $C_1 = 6.3$ ,  $g_2 = 58\text{MPa}$ ,  $C_2 = 95.0$ )

In Equation (3), which expresses the level of latent-hardening, the value of  $q$  for fcc metals is often assumed to be in the range 1.0 to 1.4. However, in the present study, we adopted 1.0 assuming that bcc metals would be more isotropic than fcc metals. In addition, we used 24 slip systems of the  $\{110\} \langle 111 \rangle$  and  $\{112\} \langle 111 \rangle$  types.

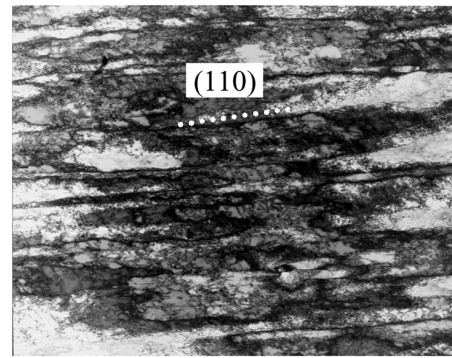
The analysis results are presented in Fig. 6. The test results obtained with  $\{110\} \langle 001 \rangle$  specimens naturally had sufficient accuracy since they were used to determine the material parameters. However, it was found that the test results shown in Fig. 1 could be reproduced with relatively high accuracy even under other test conditions using the same material constant but different crystal orientations. In the experiment, the  $\{110\} \langle 112 \rangle$  and  $\{110\} \langle 557 \rangle$  specimens showed a two-stage hardening behavior. In this respect, it was found that in the crystal plasticity analysis too, the two-stage hardening phenomenon could be reproduced, although the amount of strain causing the transition was not the same.

As described above, by using the crystal plasticity model, which takes into consideration the interaction between slip systems, it was found possible to reproduce the complicated change in work hardening behavior of crystals at large strains that are dependent on crystal orientation.

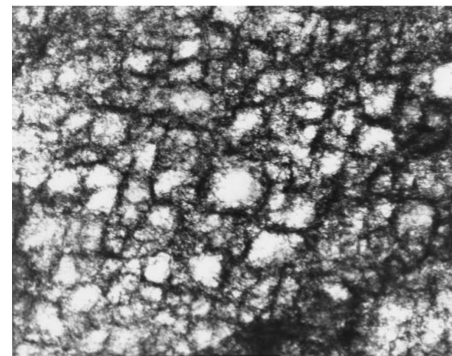
#### 4. Results of Observation of Dislocation Structure after Deformation

There is a good possibility that the complicated work hardening behavior of ferritic single crystal at large strains that we have seen so far was not only due to the activities of slip systems, which differ according to test conditions, but also due to the interaction between slip systems. Therefore, with the aim of understanding the interaction between slip systems more directly, we observed dislocation structures after the simple shear tests by using a transmission electron microscope (TEM).

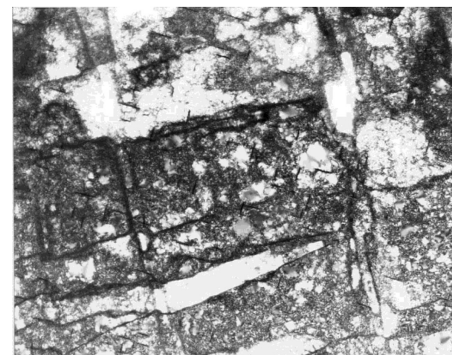
Fig. 7 shows the observation results obtained with  $\{111\} \langle 112 \rangle$ ,



(a)  $\{111\} \langle 112 \rangle$  60%



(b)  $\{100\} \langle 001 \rangle$  15%



(c)  $\{100\} \langle 011 \rangle$  60%

Fig. 7 Dislocation structure in single crystals: (a) at 60% strain for  $\{111\}$  normal direction and  $\langle 112 \rangle$  shear direction, (b) at 15% strain for  $\{100\}$  normal direction and  $\langle 001 \rangle$  shear direction and (c) at 60% strain for  $\{100\}$  normal direction and  $\langle 011 \rangle$  shear direction

$\{100\} \langle 001 \rangle$ , and  $\{100\} \langle 011 \rangle$  specimens. The  $\{111\} \langle 112 \rangle$  specimen revealed one set of dislocation boundaries parallel with the (110) plane (Fig. 7 (a)). This type of dislocation structure is often observed in  $\gamma$ -fibers of interstitial-free (IF) steel.<sup>4,5)</sup> On the other hand, the  $\{100\} \langle 001 \rangle$  specimen showed a nondirectional dislocation cell structure (Fig. 7 (b)), and the  $\{100\} \langle 011 \rangle$  specimen revealed a structure with two sets of parallel dislocation boundaries (Fig. 7 (c)). Several studies have reported the relationship between crystal orientation and dislocation structure. As for bcc steel, it is reported that the observed

microstructures of hot rolled IF steel after uniaxial tensile deformation might be classified into several types, which are one set of parallel dislocation boundaries, two sets of parallel dislocation boundaries and equiaxed cells and the type of microstructure has a close relationship with the grain orientation.<sup>6)</sup> The observed microstructures shown in this study can be classified similarly.

The formation of the dislocation structure is the result of interactions among many dislocations. However, it can be considered, that the above difference in the form of a dislocation structure has something to do with the fact that the slip systems that can be active under given boundary conditions are limited. Therefore, we made an in-depth analysis of the crystal plasticity analysis results described above to determine the slip systems that were active under specific test conditions. As a result, under the  $\{111\} \langle 112 \rangle$  condition in which one set of dislocation boundaries structure was formed (Fig. 7 (a)), it was found that two slip systems are active in the early stages and that they share one slip plane. Under the  $\{100\} \langle 001 \rangle$  condition in which an equiaxed cell structure was formed (Fig. 7 (b)), four slip systems are active and their slip planes are different from one another.

On the other hand, under the  $\{100\} \langle 011 \rangle$  condition in which two sets of dislocation boundaries are formed (Fig. 7 (c)), four slip systems are active, but they belong to two slip planes. Namely, there is correlation between the calculated number of slip systems, especially slip planes, obtained in the crystal plasticity analysis and the type of dislocation structure shown in Fig. 7. Generally speaking, the work hardening behavior of a material is governed by the total sum of slip rates of the active slip systems and the mean free path of dislocations. When the total sum of slip rates remains almost the same, it is considered that the mean free path corresponds well to the work hardening behavior. According to the results of the present study, the mean free path can be reasonably estimated to be the largest in the structure of one set of parallel dislocation boundaries, the smallest in that of equiaxed cells and intermediate in that of two sets of parallel dislocation boundaries.

Looking at the relationship between the actual work hardening behavior and dislocation structure, the order in terms of work hardening rate is this: cell structure > two-directional dislocation wall > one-directional dislocation wall. This agrees well with the magnitude of the mean free path of dislocations estimated from the results of observed dislocation structures. With the  $\{100\} \langle 001 \rangle$  specimen, it was impossible to give a deformation beyond 15%. The reason this is considered is because the presence of many active slip systems, which made dynamic recovery difficult and prevented new mobile dislocations from being introduced into the crystal, causing the crystal to lose its work hardenability. As described above, we found that there is a good possibility that the work hardening behavior, which is dependent on the crystal orientation can be correlated to the formation of a characteristic dislocation structure via the presence of active slip systems and the interaction between them. Concerning the correlation with the microscopic change in the structure, we shall discuss it in detail in the future.

Of the specimens that showed a two-stage hardening behavior, the dislocation structure of  $\{110\} \langle 112 \rangle$  specimen was observed. Fig. 8 shows the results of the observation of the dislocation structures formed in that specimen at a shear strain of 15% and 60%, respectively. It was found that when the shear strain was 15%, one-directional dislocation boundaries parallel with the  $(2\bar{1}1)$  plane is being formed. This result corresponds to the result obtained with  $\{111\} \langle 112 \rangle$  specimen, which formed one-directional dislocation boundaries before the two-stage work hardening shown in Fig. 2. On

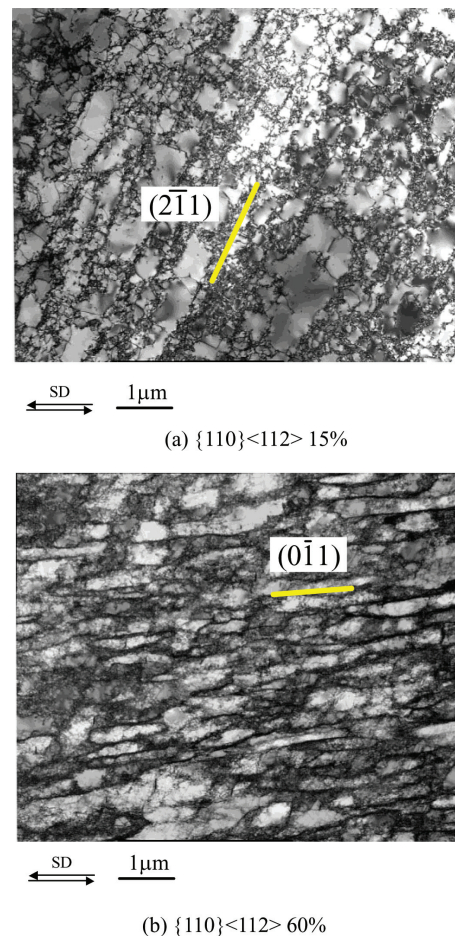


Fig. 8 Dislocation structure in single crystals: (a) at 15% strain for  $\{110\}$  normal direction and  $\langle 112 \rangle$  shear direction and (b) at 60% strain for  $\{110\}$  normal direction and  $\langle 112 \rangle$  shear direction

the other hand, when the shear strain was 60%, not only the dislocation boundaries parallel with the  $(2\bar{1}1)$  plane, but also dislocation boundaries parallel with the  $(0\bar{1}1)$  plane was observed. This is considered to suggest the presence of interactions between two or more slip systems in the final stage of deformation. Probably because of such an interaction between slip systems, the behavior of the  $\{110\} \langle 112 \rangle$  specimen, shown in Fig. 2, differs from that of the  $\{111\} \langle 112 \rangle$  specimen and gradually comes to resemble the work hardening behavior of the  $\{100\} \langle 011 \rangle$  specimen that forms two sets of dislocation boundaries.

What then causes such a transition of slip systems? A specimen with plane normal of  $\{110\}$  was subjected to crystal orientation measurement by electron backscattering pattern (EBSP) after a simple shear test and the rotation angle produced by the simple shear deformation was evaluated. The evaluation results are shown in Fig. 9. It was found that the  $\{110\} \langle 557 \rangle$  and  $\{110\} \langle 112 \rangle$  specimens that had showed two-stage hardening behavior had a large rotation angle, whereas the rotation angle of the  $\{110\} \langle 001 \rangle$  specimen was minimal. These results and the results shown in Fig. 8 suggest that under those test conditions, the simple shear produces a large crystal rotation angle from active slip systems, causing a transition of the slip systems to occur. Namely, it is considered that since the dislocations introduced by the predominant slip systems become latent, which

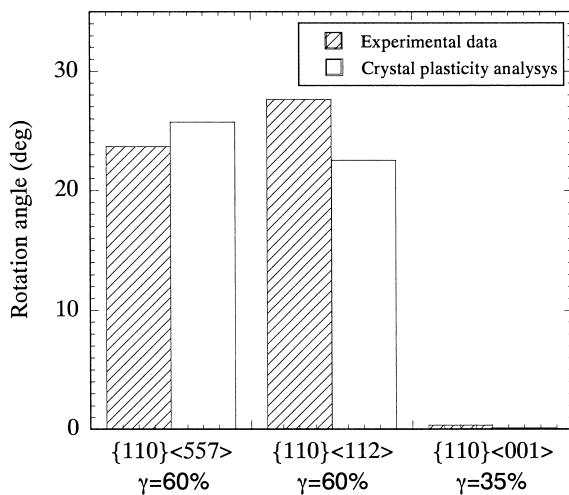


Fig. 9 Crystal rotation angle after shear deformation

interact strongly with the dislocations introduced by new active slip systems and then the work hardening rate increases from halfway, showing a two-stage hardening behavior.

Fig. 9 also shows the crystal rotation angles obtained by our crystal plasticity analysis under various conditions. It can be seen that the analysis results agree well with the experimental results. In the crystal plasticity analysis as well, a two-stage hardening behavior could be reproduced as shown in Fig. 6. This is considered due to the fact that as in the experiment, the slip systems in the early stages of deformation and the new slip systems that are activated by a crystal rotation interact with each other as per Equation (2).

## 5. Conclusion

We studied the work hardening behavior of ferritic single crystal at large strains and its relationship with the crystal orientation. As a result, it was found that the work hardening behavior varies markedly according to the activity of slip systems and the interaction between them. It was also found that the dislocation structure of the material

after deformation shows several characteristic forms, which depend on the selection of slip systems and the work hardening behavior of crystals.

Crystal plasticity analysis is a technique, which permits analyzing a macroscopic deformation behavior with the shear deformation of each slip system as the elementary process and with consideration given to the interaction between those slip systems. The present study applied the technique to analyze the behavior of single crystals at large strains and showed that the technique has a high degree of prediction accuracy. Formerly, compared with the phenomenological theory of plasticity that uses yield functions, crystal plasticity analysis had limited applications because of the huge computing load. With the recent progress of computer technology, however, the problem is rapidly being solved.

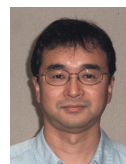
In order to respond the expectations for advanced materials in the future, it is necessary to further enhance the performance of the existing technique. We intend to study the technique as an effective tool for exploring the microscopic and macroscopic worlds, and thereby develop new materials and new application technologies in order to meet the increasingly sophisticated customer needs.

## References

- 1) Hu, Z., Rauch, E. F., Teodosiu, C.: Int. J. Plasticity. 839, 8 (1992)
- 2) Teodosiu, C., Hu, Z.: Proc. of Numiform '95 on Simulation of Materials Processing: Theory, Methods and Applications, Balkema, Rotterdam, 1995, p.173
- 3) Rauch, E. F.: Mat. Sci. Eng. A241, 179 (1998)
- 4) Nesterova, E., Bacroix, B., Teodosiu, C.: Mat. Sci. Eng. A309-310, 495 (2001)
- 5) Nesterova, E., Bacroix, B., Teodosiu, C.: Met. Mat. Trans. A. 32A, 2527 (2001)
- 6) Uenishi, A., Teodosiu, C., Nesterova, E. V.: Mat. Sci. Eng. A400-401, 499 (2005)
- 7) Bouvier, S., Haddadi, H., Levee, P., Teodosiu, C.: J. Mat. Proc. Tech. 96, 172 (2006)
- 8) Suzuki, N. et al.: Plasticity and Working. 46 (534), 636-640 (2005)
- 9) Keh, A. S.: Phil. Mag. 9, 12 (1965)
- 10) Kuroda, M., Shizawa, K.: Plasticity and Working. 43 (495), 299-309 (2002)
- 11) Asaro, R. J., Needleman, A.: Acta Metal. 33, 923-953 (1985)
- 12) Isogai, E. et al.: Collection of Papers for FY2009 Spring Lecture Meeting on Plastic Working. 2009, p. 207-208



Akihiro UENISHI  
Senior Researcher, Dr.  
Forming Technologies R&D Center  
Steel Research Laboratories  
20-1, Shintomi, Futtsu, Chiba 293-8511



Yoichi IKEMATSU  
General Manager, Dr.Eng.  
Hirohata R&D Lab.



Eiji ISOGAI  
Senior Researcher  
Hirohata R&D Lab.



Masaaki SUGIYAMA  
Chief Researcher, Dr.Eng.  
Materials Characterization Research Lab.  
Advanced Technology Research Laboratories



Natsuko SUGIURA  
Senior Researcher, Dr.Eng.  
Kimitsu R&D Lab.



Shunji HIWATASHI  
General Manager, Dr.  
Nagoya R&D Lab.